Published by IOP Publishing for Sissa Medialab

Received: *October 15, 2019*
Revised: *February 1, 2020*
Accepted: *March 4, 2020*
Published: *April 6, 2020*

21st International Workshop on Radiation Imaging Detectors
7–12 July 2019
Crete, Greece

Localization of radioactive source using a network of small form factor CZT sensors

G. Fragkos,[a] **K. Karafasoulis,**[b] **A. Kyriakis**[c,1] **and C. Potiriadis**[d]

[a] *Hellenic Army General Staff R&IT Directorate (HAGS/R&IT Dir), Mesogeion Ave. 227-231, 15561, Holargos, Athens, Greece*
[b] *Hellenic Army Academy, Vari, Attiki, 16673 Greece*
[c] *Institute of Nuclear Physics, National Center for Scientific Research Demokritos, Patriarxou Grigoriou & Neapoleos, Agia Paraskevi — Attiki, 15341 Greece*
[d] *Greek Atomic Energy Commission, Patriarxou Grigoriou & Neapoleos, Agia Paraskevi — Attiki, 15341 Greece*

E-mail: kyriakis@inp.demokritos.gr

Abstract: We present a small factor ($0.5\,\mathrm{cm}^3$) CZT static sensor network consisted of a number of Non-Directional Detectors (NDD) capable to localize bare and lightly shielded radiation sources. The localization is performed with a fusion algorithm based on a fast analytical technique. The algorithm has been tested using simulated data and verified with experimental data from a static ^{137}Cs source of 7 MBq. The localization accuracy of the order of 15 cm has been archived in 3D for bare sources and of the order of 20 cm in 2D for light shielded sources within a monitored volume of $5\,\mathrm{m} \times 2.8\,\mathrm{m} \times 2\,\mathrm{m}$.

Keywords: Radiation monitoring; Search for radioactive and fissile materials

[1] Corresponding author.

https://doi.org/10.1088/1748-0221/15/04/C04015

Contents

2020 JINST 15 C04015

1 Introduction

In the new era of homeland security there is a growing concern regarding the possession and the potential use of radiological materials by terrorist groups usually in the form of a radiological dispersion device *(RDD)*, also known as *"dirty bomb"*. Since the defended areas from such a threat may not have specific entrance and exit points, the problem of how to localize and identify a radioactive source in an open area should be investigated. The detection has to overcome a variety of uncontrollable factors, such as the presence of benign sources, time and space varying background noise, and obstacles that may occlude signal from sources.

Several researchers have addressed the problem of radiation source localization using approaches that vary from geometric difference triangulation [1] to Bayesian algorithms that calculate the posteriori probability distribution based on prior estimates [2]. The Ratio of Square Distance (ROSD) method introduced in [3], presents a closed form solution which can solve the imaginary root problem, when dealing with more than 3 sensors. Maximum Likelihood Estimation (MLE) has been used successfully [4] to estimate the parameters of multiple radiation sources as well. It follows a grid-based approach and it is computationally expensive and thus unsuitable for real time applications [2]. A Particle filter algorithm was suggested in [5], where it has been used in a border monitoring scenario. Twelve 2 in$\times$2 in. NaI detectors deployed in a monitoring region of 42×42 m^2. The networked algorithm was able to detect the source meters before entering the monitoring region.

We tackled the above complicated problem using a network of small form factor spectroscopic detectors (Non-Directional Detectors — NDD) realized using CZT crystals. The capabilities of the above NDD network to localize radioactive sources were investigated using simulated data produced by GEANT4 [6] software via the SWORD (SoftWare for Optimization of Radiation

Detectors) package [7]. Then a series of verification tests were performed using experimental data collected by a locally developed data acquisition system from the CZT sensor network realized in our lab using both bared and light shielded sources. The localization algorithm was based on a fast analytical technique.

This article is organized as follows: in section 2 the simulation of NDD system is presented, in section 3 the evaluation of the algorithm using simulated data is discussed, in section 4 the experimental setup and the verification experiments with the collected real data are described followed by the conclusions in section 5.

2 Sensor network simulation

2.1 Geometrical setup of the simulation

Detailed simulation has been used to study the ability of the NDD network to localize a radiation source within a volume of 28 m^3. A model of five (5) CZT spectroscopic sensors in cruciform planar topology (figure 1) each having an active volume of 0.5 cm^3 has been irradiated by a ^{137}Cs source (activity 37 MBq) for 45 sec with air as intermediate medium in the absence of NORM background. The inter-sensor distance in the horizontal axis was set to 2.5 m whilst the vertical distance of the sensors was set to 1.4 m. This setup was selected to match with our experimental hall specification (see section 4) with dimension 5 m (length) × 2 m (width) × 2.8 m (height). The source has been placed at various positions at planes parallel to the sensor plane at distances between 40 cm to 200 cm away from the sensor plain in steps of 40 cm.

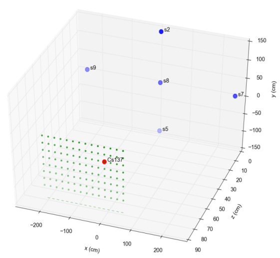

Figure 1. Simulation setup up with sensors (blue points) in cruciform planar topology. The energy response of the sensors has been recorded when a radioactive source i.e. ^{137}Cs (in red) has been placed in various position (in green) at planes parallel to the sensor plane.

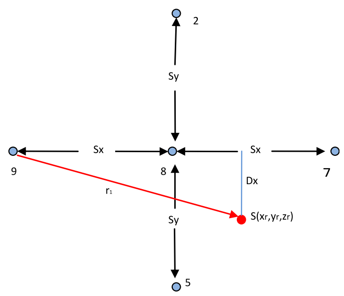

Figure 2. The "Cruciform 5 sensor topology" with a radiation source placed at (x_r, y_r, z_r). The horizontal intersensor distance is S_x, while the vertical intersensor distance is S_y

For each source position, the energy response of each sensor has been recorded separately and then the energy responses of the 5 sensors were merged. This approach was much faster than simulating the response of all the 5 sensors concurrently within the monitoring volume of 28 m^3 on the penalty of loosing part of the scattered radiation which we believe to be negligible in first approximation. The sensor identification number was set to 2 for upper central sensor, 5 for bottom central sensor, 7, 8 and 9 for the three inline sensors respectively (figure 1), whilst the radiation source, R, was set at points $\left(X_R^j, Y_R^j, Z_R^j, j = 1, 3000\right)$ for a given plain as can be seen indicatively in figure 1.

2020 JINST 15 C04015

2.2 Localization algorithm

Although the energy spectra, $E_i^{\Delta t}\left(X_R^j, Y_R^j, Z_R^j\right), i = 1,5$, of each sensor is recorded, for the same time window Δt this work uses only the total recorded counts. This is done to increase the sensors' sensitivity by taking into account not only the photo-peak information but the scattered radiation as well. The localization of the radiation source algorithm has been designed to handle sources independent of their activity.

An approach for the fusion algorithm based on an analytical procedure has been developed for the "Cruciform 5 Sensor topology" (figure 2). Taking into account that the total counts, $A_i, i = 1,5$, recorded by each sensor is inversely proportional to the square of the source-sensor distance, r_i^2, $i = 2,5,7,8,9$ we have:

$$q_1^x = \frac{r_9^2}{r_8^2} = \frac{A_8}{A_9} = \frac{(S_x + x_r)^2 + D_x^2}{x_r^2 + D_x^2}, q_2^x = \frac{r_7^2}{r_8^2} = \frac{A_8}{A_7} = \frac{(S_x - x_r)^2 + D_x^2}{x_r^2 + D_x^2}, D_x^2 = \frac{2S_x x_r + S_x^2}{q_1^x - 1} - x_r^2$$

Thus

$$x_r = \frac{S_x(q_1^x - q_2^x)}{2\left(q_1^x + q_2^x\right) - 4} \tag{2.1}$$

Similarly,

$$q_1^y = \frac{r_2^2}{r_8^2} = \frac{A_8}{A_2} = \frac{\left(S_y + y_r\right)^2 + D_y^2}{y_r^2 + D_y^2}, q_2^y = \frac{r_5^2}{r_8^2} = \frac{A_8}{A_5} = \frac{\left(S_y - y_r\right)^2 + D_y^2}{y_r^2 + D_y^2}, D_y^2 = \frac{2S_y y_r + S_y^2}{q_1^y - 1} - y_r^2$$

And

$$y_r = \frac{S_y(q_1^y - q_2^y)}{2\left(q_1^y + q_2^y\right) - 4} \tag{2.2}$$

In addition the depth source coordinate, z_r, can be estimated as the average of

$$z_r = \frac{z_r^1 + z_r^2}{2}, \text{ where } z_r^1 = \sqrt{D_x^2 - y_r^2}, z_r^2 = \sqrt{D_y^2 - x_r^2} \tag{2.3}$$

In cases where one of the z_r^1 or z_r^2 is not defined, $z_r = z_r^2$ or $z_r = z_r^1$ respectively.

3 Evaluation of localization algorithm

The source localization accuracy was tested using simulated data produced in the way described in section 2.1. The results using the analytical localization algorithm described in section 2.2 are shown in figures 3, 4. In figure 3 the plot of the horizontal ($X_{\text{Calculated}} - X_{\text{True}}$) and vertical ($Y_{\text{Calculated}} - Y_{\text{True}}$) position distributions are shown with an estimated accuracy (standard deviation of the distribution) of less than 15 cm whilst in figure 4 the plot of the depth position distribution ($Z_{\text{Calculated}} - Z_{\text{True}}$) is shown with an accuracy of less than 18 cm. A systematic error of less than 15 cm is observed in the depth source position. This is due to the fact that the analytical method does not take into account the geometrical form factors of the sensors and the radiation attenuation of the medium between the source and the sensors (in general unknown parameters).

This leads to an underestimation of the counts recorded by the sensors. A test has been performed by correcting each sensor response using the true source position, a process that significantly eliminates this systematic error. To cope with this problem an approach based on Multivariate Analysis techniques could be applied. This will be a subject of a future work.

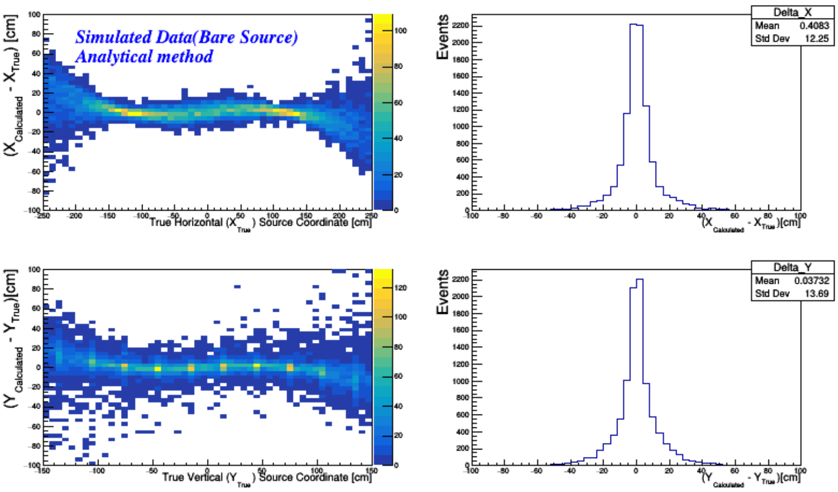

Figure 3. Horizontal and Vertical source position distributions for the simulated "Cruciform 5 Sensor topology". For the simulation a ^{137}Cs source (37 MBq) was used at various distances from the sensor plain that radiated for 45 sec. The corresponding accuracies (standard deviation) are also shown.

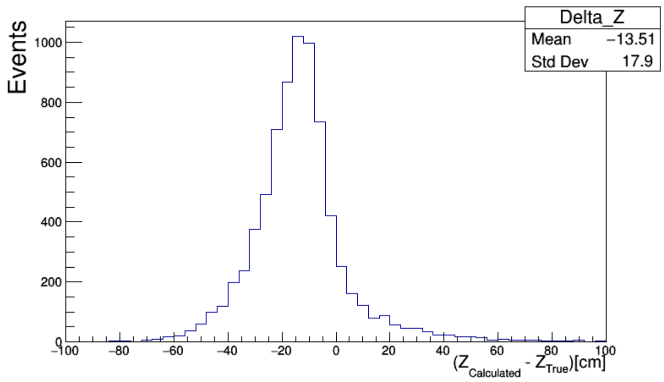

Figure 4. Depth position distribution for the simulated "Cruciform 5 Sensor topology". For the simulation a ^{137}Cs source (37 MBq) was used at various distances from the sensor plain that radiated for 45 sec. The corresponding accuracy (standard deviation) is also shown.

4 Experimental setup

4.1 Source position platform

For the verification of the data fusion algorithms a testbed was setup using CZT detectors purchased by RITEC [8]. A 3-D step-motor rail system based on an Arduino microcontroller [9] and controlled via a java GUI software, positions a radioactive source in predefined locations. This system has been developed and installed in the testbed area (figure 5).

The spectral response of the "Cruciform 5 sensor topology" system can be seen in figure 6 for a bare ^{137}Cs source of activity 7 MBq and exposure time of 3 min whilst the corresponding spectra for the above source inside a cylinder of 1 cm width (light shielded source) can be seen in figure 7. The absence of the X-ray 32 keV is clear. In both cases the background was subtracted.

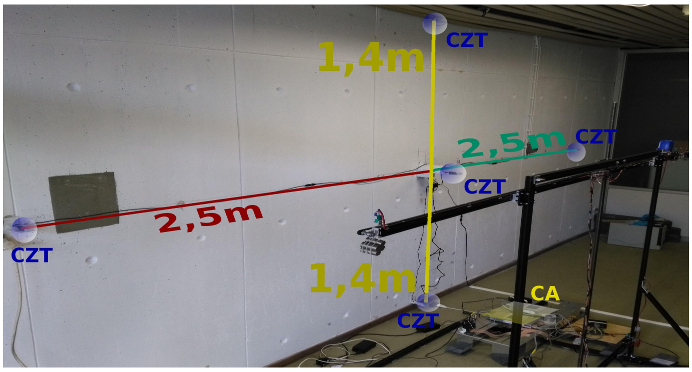

Figure 5. Experimental Setup with a 3D step motor system that positions the radioactive Source (blue box) in the appropriate position. Five sensors in cruciform topology have been mounted on the wall (transparent circles).

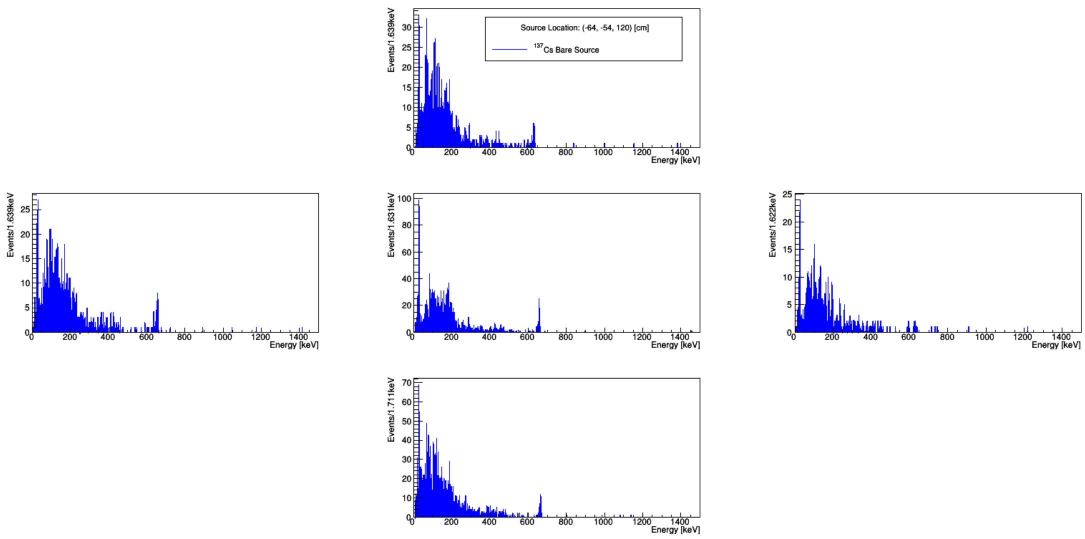

Figure 6. The spectral response of the "Cruciform 5 sensor topology" system for the bare ^{137}Cs, source of activity 7 MBq and exposure time of 3 min. A clear X-ray peak at 32 keV is observed.

The DAQ system is based on a client-server architecture. The software for the fusion node utilizes web technologies [10] which makes it possible for the sensors, the fusion node, and the operator to be at different locations.

4.2 Experimental Spatial accuracy for the bare source using analytical method

The analytical method described in section 2.2 has been applied in the experimental setup. The source localization accuracy was tested using a bare ^{137}Cs source with activity of 7 MBq and exposure time of 3 min. The spatial position distributions for a bare source at a distance of 120 cm from the sensor plain is shown in figure 8 and a spatial localization accuracy of less than 15 cm was calculated. The systematic error in depth coordinate could be explained as in section 3.

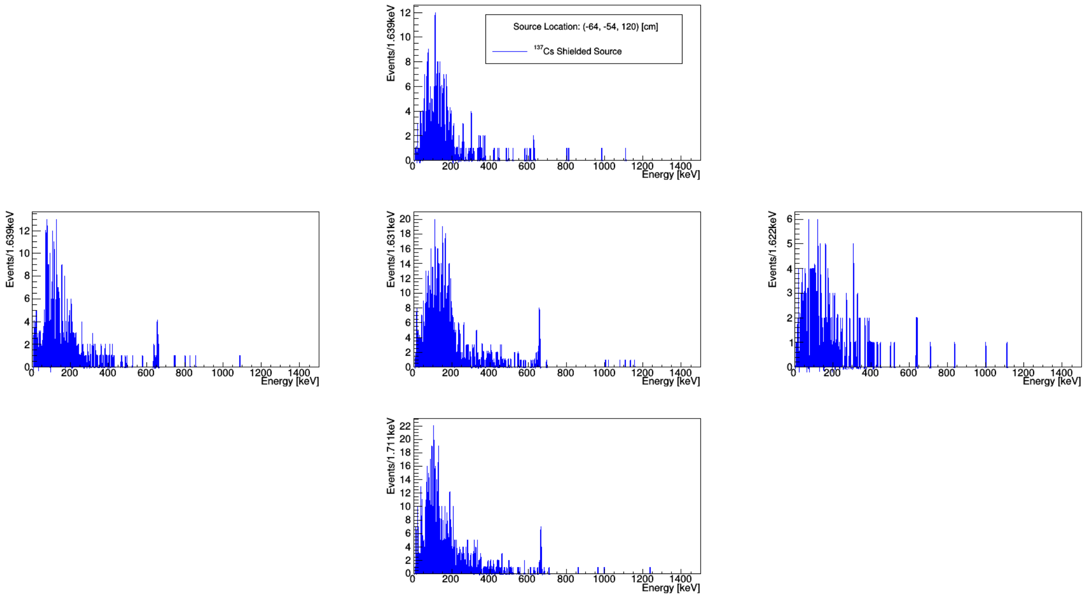

Figure 7. The spectral response of the "Cruciform 5 sensor topology" system for the light shielded ^{137}Cs source of bare activity 7 MBq and exposure time of 3 min. No X-ray peak is observed any more at 32 keV.

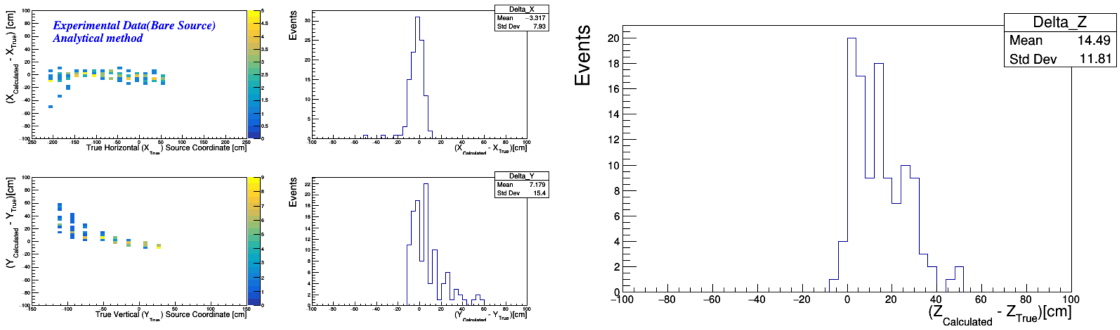

Figure 8. Experimental "Cruciform 5 Sensor topology" with a bare ^{137}Cs Source (7 MBq) at a distance 120 cm from the sensor plain that radiated for 3 min using analytical method, (Left) Horizontal and Vertical source position distributions, (Right) Depth source position distribution. The corresponding accuracies are shown as well.

4.3 Experimental Spatial accuracy for the light shielded source using analytical method

In case of the light shielded source the depth coordinate was not possible to be calculated correctly. Thus after processing the spectra in the central computing station using the analytical algorithm, the location of the radioactive material was estimated with an accuracy better than 20 cm in horizontal and vertical directions for an exposure time of at least 40 sec as can be seen in figure 9.

5 Conclusions

The ability of a sensor network consisting of five small form factor CZT sensors having a coplanar cruciform topology has been evaluated using a fast analytical method on fully simulated data samples

2020 JINST 15 C04015

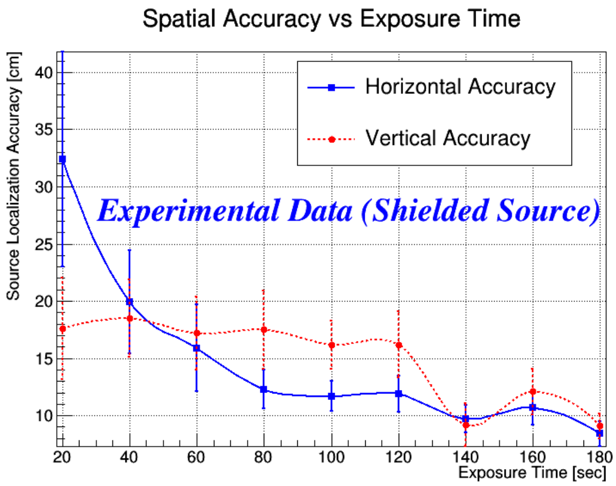

Figure 9. Horizontal (blue) and vertical (red) source position accuracy of the light shielded ^{137}Cs radioactive source as a function of the exposure time.

of ^{137}Cs radiation source in 3D. The algorithm has been verified by a series of experiments, where the CZT sensor network has been irradiated by a bare ^{137}Cs Source (activity 7 MBq). Localization accuracy within a volume of 5 m$\times$2.8 m$\times$2 m of ~ 15 cm in 3D has been achieved after an exposure of 3 min. On the contrary the same source with a light shield (inside a Pb cylinder of 1 cm width) can be localized in 2D with a accuracy of less than 20 cm after an exposure time of 40 sec whilst the depth can't be estimated with a reasonable accuracy.

Acknowledgments

This research has been funded by NATO (SfP-984705) SENERA project.

References

[1] C. Wu, S. Sen, N. Rao and R. Brooks, *Efficient network detection of radiation sources using localization*, presented at *IEEE Nuclear Science Symposium*, Seattle, WA, U.S.A., 8–15 November 2014.

[2] A.H. Liu, J.J. Bunn and K.M. Chandy, *Sensor networks for the detection and tracking of radiation and other threats in cities*, in proceedings of the *10th International Conference on Information Processing in Sensor Networks*, Chicago, IL, U.S.A., 12-14 April 2011, pp. 1–12.

[3] J.-C. Chin, N.S.V. Rao, D.K.Y. Yau, M. Shankar, Y. Yang, J.C. Hou et al., *Identification of low-level point radioactive sources using a sensor network*, *ACM Trans. Sensor Networks* **7** (2010) 1.

[4] M. Morelande, B. Ristic and A. Gunatilaka, *Detection and parameter estimation of multiple radioactive sources*, in proceedings of the *10th International Conference on Information Fusion*, Quebec, Que., Canada, 9–12 July 2007, pp. 1–7.

[5] N.S. Rao, S. Sen, N.J. Prins, D.A. Cooper, R.J. Ledoux, J.B. Costales et al., *Network algorithms for detection of radiation sources*, *Nucl. Instrum. Meth.* **A 784** (2015) 326.

[6] GEANT4 collaboration, *GEANT4: A Simulation toolkit*, *Nucl. Instrum. Meth.* **A 506** (2003) 250.

2020 JINST 15 C04015

[7] Oak Ridge National Laboratory, *RSICC CODE PACKAGE CCC-7676*, http://www-rsicc.ornl.gov/codes/ccc/ccc7/ccc-767.html (2012).

[8] RITEC, *Gamma-Radiation CdZnTe Microspectrometer*, http://www.ritec.lv/files/uspec/R_uSPEC_A4_v5b.pdf.

[9] Arduino Uno Homepage, https://www.arduino.cc/.

[10] *WildFly a flexible, lightweight, managed application runtime*, http://wildfly.org/.